Inorg. Chem. **2006**, *45*, 9064–9074

Synthesis, Solid-State NMR, and X-ray Powder Diffraction Characterization of Group 12 Coordination Polymers, Including the First Example of a C-Mercuriated Pyrazole

Norberto Masciocchi,*,† Simona Galli,† Enrica Alberti,† Angelo Sironi,‡ Corrado Di Nicola,§ Claudio Pettinari,*,§ and Luciano Pandolfo||

Dipartimento di Scienze Chimiche e Ambientali, Università dell'Insubria, via Valleggio 11, 22100 Como, Italy, Dipartimento di Chimica Strutturale e Stereochimica Inorganica, Università di Milano, via Venezian 21, 20133 Milano, Italy, CIMAINA, via Celoria 16, 20133, Milano, Italy, Dipartimento di Scienze Chimiche, Università di Camerino, via S. Agostino 1, 62032 Camerino (MC), Italy, and Dipartimento di Scienze Chimiche, Università di Padova, via Marzolo 1, 35131 Padova, Italy

Received July 20, 2006

Cadmium and mercury acetates have been reacted with pyrazole (Hpz) and 3,5-dimethylpyrazole (Hdmpz), affording distinct mixed-ligand species, selectively prepared upon slightly modifying the reaction conditions. Two polymorphs of $[\{Cd(\mu\text{-ac})_2(Hpz)_2\}_n]$, as well as the $[\{Cd(\mu\text{-ac})_2(Hdmpz)_2\}_n]$ species (Hac = acetic acid), were obtained by solution chemistry, while the two-dimensional $[\{Cd_3(\mu_3\text{-ac})_4(\mu\text{-pz})_2(Hpz)_2\}_n]$ and $[\{Cd(\mu\text{-ac})(\mu\text{-pz})\}_n]$ polymers were prepared upon controlled thermal treatment of one of the $[\{Cd(\mu\text{-ac})_2(Hpz)_2\}_n]$ forms. Two mercury derivatives, $[\{Hg_3(\mu\text{-ac})_3(\mu\text{-pz})_3\}_n]$ and $[\{Hg(ac)(\mu\text{-dmpz})\}_n]$, were also prepared, the latter containing one-dimensional chains of Hg(II) ions bridged by C-mercuriated Hdmpz ligands. All their crystal structures (but one) were determined by powder diffraction methods using conventional X-ray laboratory equipment, supported by ^{13}C CPMAS NMR measurements. The latter method helped in assigning a C-metalated nature to an amorphous material of [Hg(ac)(pz)] formula, obtained by employing EtOH as a solvent. A few other Hdmpz-containing cadmium acetates were also prepared, but their polyphasic nature, evidenced by diffraction methods, hampered their complete structural characterization.

Introduction

In recent years, (poly)carboxylates and anionic diazaaromatic compounds have been widely employed in the construction of coordination polymers, in search for functional materials possessing magnetic, optical, thermal, anticorrosive, and even antibacterial activity.[1] A vast portion of these studies has been devoted to the preparation of stable, porous metal−organic frameworks (MOF's), capable of ion pair and molecule recognition and gas and liquid sorption[2] and, possibly, showing high gas-storage capacity for environmentally friendly energetic processes.[3] The pioneering work by Yaghi[4] demonstrated how, with complex polycarboxylates, crystal engineering techniques can be successfully applied to the preparation of second-generation functional MOF's and indicated that aromatic linkers, together with carboxylates, grafting onto transition metal ions (such as copper and zinc), are highly efficient building blocks. However, the recent reports on the gas-sorption properties and performances of very simple binary compounds, such as $[Mn(HCOO)_2]$,[5] $[\{Cu(pz)_2\}_n]$,[6] and $[\{M(C_4H_3N_2O)_2\}_n]$

* To whom correspondence should be addressed. E-mail: norberto.masciocchi@uninsubria.it.
† Università dell'Insubria.
‡ Università di Milano and CIMAINA.
§ Università di Camerino.
|| Università di Padova.

(1) Janiak, C. *Dalton Trans.* **2003**, 2781.
(2) Tabares, L. C.; Navarro, J. A. R.; Salas, J. M. *J. Am. Chem. Soc.* **2001**, *123*, 383.
(3) Eddaoudi, M.; Li, H.; Yaghi, O. M. *J. Am. Chem. Soc.* **2000**, *122*, 1391. Snurr, R. Q.; Hupp, J. T.; Nguyen, S. *AIChE J.* **2004**, *50*, 1090.
(4) Rosi, N. L.; Eckert, J.; Eddaoudi, M.; Vodak, D. T.; Kim, J.; O'Keeffe, M.; Yaghi, O. *Science* **2003**, *300*, 1629.
(5) Dybtsev, H. N.; Chun, H.; Yoon, S. H.; Kim, D.; Kim, K. *J. Am. Chem. Soc.* **2004**, *126*, 32.
(6) Cingolani, A.; Galli, S.; Masciocchi, N.; Pandolfo, L.; Pettinari, C.; Sironi, A. *J. Am. Chem. Soc.* **2005**, *127*, 6144.

10.1021/ic061349b CCC: $33.50
Published on Web 10/04/2006

(M = Cu, Pd),[7] opened the way to the preparation of porous materials in which the length of the linker is highly reduced and the dimensionality of the derived polymer is changed. Thus, simple monocarboxylates and exo-bidentate anionic azoles may be easily employed, without the need of synthesizing expensive and complex aromatic carboxylates with polyfused rings.

In previous papers of ours, we have shown the unexpected formation of a new polymorph of the monodimensional copper pyrazolate polymer from copper−carboxylate precursors, possessing interesting vapochromic behavior,[6] as well as zinc complexes containing pyrazolates or a mixture of pyrazolates and acetates, highlighting their competition in the formation of polymeric species.[8] In this paper we have further extended these latter studies, and we present the preparation, characterization, and structural models of a number of cadmium- and mercury-containing acetate/pyrazolate species, including a rare example of a polymer built by C-mercuriated pyrazoles.

For the sake of simplicity, all the species discussed below are here reported with their numbering scheme (Hpz = pyrazole, Hdmpz = 3,5-dimethylpyrazole): [{Cd(μ-ac)$_2$(Hpz)$_2$}$_n$], **1** (triclinic phase, **1a**; monoclinic phase, **1b**); [{Cd$_3$(μ_3-ac)$_4$(μ-pz)$_2$(Hpz)$_2$}$_n$], **2**; [{Cd(μ-ac)(μ-pz)}$_n$], **3**; [{Cd(μ-ac)$_2$(Hdmpz)$_2$}$_n$], **4**; [Cd(ac)$_2$(Hdmpz)$_2$]·*x*Hdmpz, **4a,b** (**a**, $x = 2$; **b**, $x = 1$); [Cd(ac)(dmpz)], **5**; [{Hg$_3$(μ-ac)$_3$(μ-pz)$_3$}$_n$], **6**; [Hg(ac)(pz)], **7**; [{Hg(ac)(μ-*C*,*N*-Hdmpz)}$_n$], **8**.

Worthy of note, the main results of this work have been achieved thanks to the extensive use of innovative ab initio laboratory X-ray powder diffraction (XRPD) methods only, which we,[9] and others,[10] have recently adopted and developed, as a fundamental structural tool in the field of coordination compounds, particularly for polymeric species containing polytopic heteroaromatic ligands.[11]

Experimental Section

Materials and Methods. All chemicals were purchased from Aldrich and used without further purification. The synthesis and recrystallization of compounds **1**−**8** were carried out in air. Elemental analyses (C, H, N) were performed with a Fisons Instruments 1108 CHNS-O elemental analyzer. IR spectra were recorded from 4000 to 100 cm^{-1} with a Perkin-Elmer System 2000 FT-IR instrument. The electrical conductances of the methanol solutions were measured with a Crison CDTM 522 conductimeter at room temperature. Positive electrospray mass spectra were obtained with a Series 1100 MSI detector HP spectrometer, using water as the mobile phase. Solutions for electrospray ionization mass spectrometry (ESI-MS) were prepared using deionized water or CH_3CN, and obtained data (masses and intensities) were compared to those calculated by using the IsoPro isotopic abundance simulator, version 2.1.[12] ^{1}H and ^{13}C NMR spectra were recorded on a Mercury Plus Varian 400 NMR spectrometer (400 MHz for ^{1}H). H and C chemical shifts are reported in ppm vs $SiMe_4$.

Synthesis of [Cd(ac)$_2$(Hpz)$_2$] (1). Dihydrated cadmium(II) acetate (0.27 g, 1.0 mmol) was dissolved in 20 mL of ethanol. To the colorless solution a pyrazole solution (0.14 g, 2.0 mmol, in 10 mL of ethanol) was added under stirring. After 2 min a colorless solid started to precipitate. The suspension was stirred for 24 h, and then the solid was filtered off, washed with 10 mL of ethanol, and dried under vacuum. Yield: 0.220 g, 60%.

1. Anal. Calcd for $C_{10}H_{14}CdN_4O_4$: C, 32.76; H, 3.85; N, 15.28. Found: C, 32.90; H, 3.96; N, 15.28. IR (Nujol, cm^{-1}): 3120 br (NH), 3108 m, 3080 w (CH), 1588 s, 1540 s br, 1400 br (CO, C···C, C···N), 490 s, 277 m. ^{1}H NMR ($CDCl_3$, 295 K): δ 2.01 (s, 6H, CH_{3ac}), 6.38 (t, 2H, 4-H$_{pz}$), 7.64 (d, 4H, 3-H$_{pz}$ or 5-H$_{pz}$). ^{1}H NMR (DMSO-d_6, 295 K): δ 1.85 (s, 6H, CH_{3ac}), 6.20 (br, 2H, 4-H$_{pz}$), 7.53 (d, 4H, 3-H$_{pz}$ or 5-H$_{pz}$), 13.8 (br, 2H, NH). ^{1}H NMR (D_2O, 295 K): δ 1.75 (s, 6H, CH_{3ac}), 6.28 (t, 2H, 4-H$_{pz}$), 7.56 (d, 4H, 3-H$_{pz}$ or 5-H$_{pz}$). ESI MS (+) (H_2O) (*m*/*z*, relative intensity %): 295, 70, [Cd(ac)(Hpz)(H_2O)$_3$]$^+$, 309, 100, [Cd(ac)(Hpz)$_2$]$^+$, 363, 45, [Cd(ac)(Hpz)$_2$(H_2O)$_3$]$^+$, 377, 20, [Cd(ac)(Hpz)$_3$]$^+$.

When the reaction was carried out in acetonitrile, the recovered yield for compound **1** was 55%. A few single crystals of the polymorph **1a** could obtained upon slow evaporation of alcoholic, hydroalcoholic, or water solutions of **1**. The polymorph **1b** was always obtained as a (microcrystalline) material when the reaction between cadmium(II) acetate and excess pyrazole was carried out in diethyl ether.

Synthesis of [Cd$_3$(ac)$_4$(pz)$_2$(Hpz)$_2$]$_n$ (2). Compound **2** has been prepared by heating compound **1b** at 110 °C for 2 h. Compound **2** is insoluble in common organic solvents and poorly soluble in water.

2. Anal. Calcd for $C_{20}H_{26}Cd_3N_8O_8$: C, 28.47; H, 3.11; Cd, 39.97; N, 13.28. Found: C, 28.34; H, 3.16; Cd, 40.5; N, 12.81. IR (Nujol, cm^{-1}): 3120 w (CH), 1548 br, 1462 m, 1400 m (CO, C···C, C···N), 660 m, 630 w, 650 w, 487 w. ^{1}H NMR (D_2O, 295 K): δ 1.75 (s, 6H, CH_{3ac}), 6.26 (t, 2H, 4-H$_{pz}$), 7.55 (d, 4H, 3-H$_{pz}$ or 5-H$_{pz}$).

Synthesis of [Cd(ac)(pz)] (3). Compound **3** has been prepared by heating compound **1b** at 170 °C for 24 h. Compound **3** is insoluble in common organic solvents and also in water.

3. Mp: 216−220 °C. Anal. Calcd for $C_{10}H_{12}Cd_2N_4O_4$: C, 25.18; H, 2.54; Cd, 47.13; N, 11.74. Found: C, 24.86; H, 2.58; N, 11.26. IR (Nujol, cm^{-1}): 3106 w (CH), 1540 sh, 1530 m, 1453 m (CO, C···C, C···N), 1050 m, 667 m, 636 w, 616 w, 461 w, 283 w.

Synthesis of [Cd(ac)$_2$(Hdmpz)$_2$] (4). Dihydrated cadmium(II) acetate (0.27 g, 1.0 mmol) was dissolved in 20 mL of ethanol. To the colorless solution a 3,5-dimethylpyrazole solution (0.19 g, 2.0 mmol, in 10 mL of ethanol) was added under stirring. After 2 min a colorless solid started to precipitate. The suspension was stirred for 24 h, and then the solid was filtered off, washed with 10 mL of a mixture of ethanol/diethyl ether, and dried under vacuum. Yield: 0.322 g, 75%.

4. Mp: 109 °C dec (see Results and Discussion). Anal. Calcd for $C_{14}H_{22}CdN_4O_4$: C, 39.77; H, 5.25; N, 13.25. Found: C, 39.94; H, 5.36; N, 13.46. IR (Nujol, cm^{-1}): 3260 sh, 3181m, 3126 m, 3086 m (NH, CH), 1600 sh, 1572 sh, 1548 s (CO, C···C, C···N), 483 m, 416 s, 352 w, 315 m, 280 m, 254 br. ^{1}H NMR ($CDCl_3$, 295 K): δ 2.04 (s, 6H, CH_{3ac}), 2.27 (s, 12H, CH_{3dmpz}), 5.85 (s, 4H, 4-H$_{pz*}$). ^{1}H NMR (D_2O, 295 K): δ 1.74 (s, 6H, CH_{3ac}), 2.04 (s, 12H, CH_{3dmpz}), 5.79 (s, 4H, 4-H$_{dmpz}$). ESI MS (+) (H_2O) (*m*/*z*,

(7) Navarro, J.; Barea, E.; Salas, J. M.; Masciocchi, N.; Galli, S.; Sironi, A.; Ania, C.; Parra, J. *Inorg. Chem.* **2006**, *45*, 2397.
(8) Cingolani, A.; Galli, S.; Masciocchi, N.; Pandolfo, L.; Pettinari, C.; Sironi, A. *Dalton Trans.* **2006**, 2479.
(9) Masciocchi, N.; Sironi, A. *Compt. Rend. Chim.* **2005**, *8*, 1617.
(10) See for example: *Powder Diffraction of Molecular Functional Materials*; Masciocchi, N., Ed.; Commission of Powder Diffraction; International Union of Crystallography: Chester, U.K., 2004; Newsletters No. 31.
(11) Masciocchi, N.; Galli, S.; Sironi, A. *Comments Inorg. Chem.* **2005**, *26*, 1.
(12) Senko, M. W. IsoPro Isotopic Abundance Simulator, v. 2.1; National High Magnetic Field Laboratory, Los Alamos National Laboratory: Los Alamos, NM.

relative intensity %): 97, 100, $[Hdmpz + H]^+$, 447, 8, $[Cd(ac)_2(Hdmpz)_2 + Na]^+$.[13]

Compound **4** can be also prepared by maintaining compounds **4a,b** (discussed below) at 110 °C for 30 min.

Synthesis of $[Cd(ac)_2(Hdmpz)_2]\cdot x$Hdmpz (4a,b) (a, $x = 2$; b, $x = 1$). Hdmpz (0.380 g, 4.0 mmol) was added to a diethyl ether suspension containing cadmium(II) acetate (0.27 g, 1.0 mmol). The suspension was stirred overnight and then filtered and washed with diethyl ether. Typical yield: 0.492 g, ca. 80%.

4a. Mp: 109 °C (dec). Anal. Calcd for $C_{24}H_{38}CdN_8O_4$: C, 46.87; H, 6.23; N, 18.22. Found: C, 47.10; H, 6.63; N, 18.44. IR (Nujol, cm^{-1}): 3195 m, 3126 m, 3096 m (NH, CH), 1592 s, 1563 s, 1411 s (CO, C···C, C···N), 483 m, 419 m, 404 w, 353 w, 342 w, 280 m br, 245 br. ^{1}H NMR (D_2O, 295 K): δ 1.75 (s, 6H, CH_{3ac}), 2.02 (s, 12H, CH_{3dmpz}), 5.78 (s, 4H, 4-H_{dmpz}). ESI MS (+) (H_2O) (*m*/*z*, relative intensity %): 97, 100, $[Hdmpz + H]^+$, 447, 70, $[Cd(ac)_2(Hdmpz)_2 + Na]^+$, 461, 20, $[Cd(ac)(Hdmpz)_3]^+$, 553, 15, $[Cd_2(ac)_3(Hdmpz)(H_2O)_3]^+$ or $[Cd_2(ac)_2(dmpz)(Hdmpz)\ (H_2O)]^+$, 617, 7, $[Cd_2(ac)_4(Hdmpz)(H_2O)_2 + Na]^+$.

4b. Mp: 109 °C (dec). Anal. Calcd for $C_{19}H_{30}CdN_6O_4$: C, 43.98; H, 5.83; N, 16.20. Found: C, 43.65; H, 6.08; N, 15.99. IR (Nujol, cm^{-1}): 3181 m, 3131 m, 3091 m (NH, CH), 1592 s, 1574 s, 1557 s, 1493 m, 1415 s, 483 m, 419 m, 404 w, 353 w, 342 w, 291 w, 283 w br, 247 w br.

Compounds **4a**,**b** were typically obtained as polyphasic mixtures, containing both species as well as the $[Cd(ac)_2(Hdmpz)_2]$ polymer, **4**. Changes in the reagents ratio and reaction conditions afforded mixtures of different proportions, no systematic trend being observed. Likely, unpredictable nucleation processes are at work, which allowed the isolation of "pure" **4b** in a very occasional manner, only in *one* fortunate preparation: in this case, the complete indexing of the XRPD trace of a (purported) monophasic specimen gave a triclinic cell ($V = 1185$ Å^3, $Z = 2$, 29 non-hydrogen atoms in the asymmetric unit), with $a = 8.61$, $b = 10.93$, and $c = 14.30$ Å, $\alpha = 116.1$, $\beta = 81.5$, and $\gamma = 100.3°$, and GoF = 33.8. Structure solution by simulated annealing and Patterson methods were attempted, but no definitive model could be built. In the absence of a complete structural model for **4b**, the proposed unit cell is still provisional, but the high GoF value seems to indicate its probable correctness. In addition, this species partially transformed into a new unknown (poly)crystalline one, **4x**, during our NMR measurements, thus hampering its full ^{13}C CPMAS NMR characterization and the recovery of the precious monophasic sample.

Synthesis of [Cd(ac)(dmpz)] (5). Compound **5** has been prepared by heating compound **4** at 170 °C for 30 min. Compound **5** is insoluble in common organic solvents.

5. Mp: 180 °C dec (see Results and Discussion). Anal. Calcd for $C_7H_{10}CdN_2O_2$: C, 31.54; H, 3.78; N, 10.51. Found: C, 31.93; H, 4.00; N, 11.06. IR (Nujol, cm^{-1}): 3106 w (CH), 1579 s, 1521 m, 1400 m (C−C, C−O, C−N), 621 w, 613 w, 486 w, 440 m, 318 br, 254 br.

Also in this case, a polyphasic XRPD trace was measured, the most prominent peaks suggesting a *C*-centered monoclinic cell ($V = 3862$ Å^3, $Z = 8$, 24 non-hydrogen atoms in the asymmetric unit), with $a = 11.71$, $b = 29.46$, and $c = 11.22$ Å and $\beta = 94.1°$, but no definitive structural model could be found.

Synthesis of $[Hg_3(ac)_3(pz)_3]$ (6). Mercury(II) acetate (0.32 g, 1.0 mmol) was added to a 10 mL diethyl ether suspension of Hpz (0.14 g, 2.0 mmol). After 2 min 5 mL of MeOH was added. The suspension was stirred for 12 h, and then the solid was filtered off, washed with 10 mL of methanol, and dried under vacuum. Yield: 0.300 g, 92%. **6** is insoluble in chlorinate solvents and poorly soluble in MeCN.

6. Mp: 232 °C (dec). Anal. Calcd for $C_5H_8HgN_2O_2$: C, 18.38; H, 1.85; N, 8.57. Found: C, 18.80; H, 2.09; N, 8.81. IR (Nujol, cm^{-1}): 3250 br (OH), 3110 w (CH), 1555 sh, 1529 s, 1490 s, 1429 m (CO, C···C, C···N), 451 w, 399 w, 376 w, 310 w. ^{1}H NMR (CD_3OD, 295 K): δ 1.82 (s, 6H, CH_{3ac}), 6.69 (t, 2H, 4-H_{pz}), 7.95 (d, 4H, 3-H_{pz} or 5-H_{pz}). ESI MS (+) (CH_3CN) (*m*/*z*, relative intensity %): 269, 80, $[Hg(pz)]^+$, 328, 100, $[Hg(pz)(ac) + H]^+$, 594, 60, $[Hg_2(pz)_2(ac)]^+$, 853, 15, $[Hg_2(pz)_2(ac)_2(acH)_3(H_2O) + H]^+$, 854, 20, $[Hg_3(pz)_2(ac)_2]^+$.

Synthesis of [Hg(ac)(pz)] (7). Mercury(II) acetate (0.32 g, 1.0 mmol) was dissolved in 10 mL of ethanol. A Hpz solution (0.14 g, 2.0 mmol, in 10 mL of ethanol) was then added under stirring. After 2 min a colorless solid started to precipitate. The suspension was stirred for 24 h, and then the solid was filtered off, washed with 10 mL of ethanol, and dried under vacuum. Yield: 0.258 g, 75%. **7** is insoluble in most common organic solvents.

7. Mp: 275 °C (chars). Anal. Calcd for $C_5H_8HgN_2O_3$: C, 17.42; H, 2.34; N, 8.13. Found: C, 17.58; H, 1.95; N, 8.25. IR (Nujol, cm^{-1}): 3250 br (OH), 3110 w (CH), 1560 sh, 1531 s, 1428 m, 1402 m, 1376 m (CO, C···C, C···N), 468 w, 456 w, 358 br, 326 br, 303 m.

Synthesis of [Hg(ac)(dmpz)] (8). To a Hdmpz solution (0.19 g, 2.0 mmol, in 10 mL of acetonitrile) was added mercury(II) acetate (0.32 g, 1.0 mmol) under stirring. After 2 min a colorless solid started to precipitate. The suspension was stirred for 24 h, and then the solid was filtered off, washed with 5 mL of acetonitrile, and dried under vacuum. Yield: 0.177 g, 50%. **8** is insoluble in most common organic solvents.

8. Mp: 260 °C (chars). Anal. Calcd for $C_7H_{10}HgN_2O_2$: C, 23.70; H, 2.84; N, 7.90. Found: C, 23.78; H, 2.97; N, 7.84. IR (Nujol, cm^{-1}): 3320 (NH), 3196 br, 3118 m, 3101 m, 3032 m, 1537 s, 1396 s (CO, C···C, C···N), 430 m, 420 sh, 405 sh, 350 br, 254 m.

Single-Crystal X-ray Analysis. A small X-ray-quality crystal (0.05 × 0.10 × 0.10 mm) of **1a** was selected from the small batch available from aqueous or alcoholic crystallizations. The diffraction data were collected at 293 K on an Enraf-Nonius CAD4 automatic diffractometer equipped with Mo Kα radiation ($\lambda = 0.710\ 73$ Å) and corrected for decay (1.00−0.83) and Lorentz−polarization effects. A total of 1199 reflections were collected, all unique, in the $3 < \theta < 25.3°$ range. A semiempirical absorption correction (ψ-scan) was not possible, due to the lack of suitable sharp intense reflections with χ near 90°. Therefore, an ex-post absorption correction by Difabs[14] was computed on the isotropically refined structural model. The structure was solved by direct methods using the program SHELXS-86[15] and refined by full-matrix least-squares techniques against F^2 using SHELXL-97.[16] Further details of the crystal structure analysis can be found in Table 1.

Ab initio X-ray Powder Diffractometry. Powders of species **1b**, **2**−**4**, **6**, and **8** were gently ground in an agate mortar and then carefully deposited in the hollow of an aluminum sample holder equipped with a quartz zero-background plate (supplied by The Gem Dugout, Swarthmore, PA). Diffraction data were collected with graphite-monochromated Cu Kα radiation, in the 5−105° (2θ) range, on a Bruker AXS D8 θ:θ diffractometer. Generator set-

(13) Na^+ and K^+ adducts are common in ESI-MS spectra because O-donors ligands such as the carboxylates immediately interact and aggregate with the small quantities of Na^+ and K^+ that are always present in H_2O solvent [Slocik, J. M.; Somayajula, K. V.; Sheperd, R. E. *Inorg. Chim. Acta* **2001**, *320*, 148].

(14) Walker, N.; Stuart, D. *Acta Crystallogr.* **1983**, *A39*, 158.
(15) Sheldrick, G. M. University of Göttingen, Göttingen, Germany, 1986.
(16) Sheldrick, G. M. University of Göttingen, Göttingen, Germany, 1997.

Table 1. Crystal Data and Details of Structure Refinements for the Species [{Cd(μ-ac)$_2$(Hpz)$_2$}$_n$], **1a**,**b** (Two Polymorphs); [{Cd$_3$(μ_3-ac)$_4$(μ-pz)$_2$(Hpz)$_2$}$_n$], **2**; [{Cd(μ-ac)(μ-pz)}$_n$], **3**; [{Cd(μ-ac)$_2$(Hdmpz)$_2$}$_n$], **4**; [{Hg$_3$(μ-ac)$_3$(μ-pz)$_3$}$_n$], **6**; and [{Hg(ac)(μ-κ_C:κ_N-Hdmpz)}$_n$], **8**

param	**1a**	**1b**	**2**	**3**	**4**	**6**	**8**
method	single-cryst XRD	powder XRD	powder XRD	powder XRD	powder XRD	powder XRD	powder XRD
formula	$C_{10}H_{14}CdN_4O_4$	$C_{10}H_{14}CdN_4O_4$	$C_{20}H_{26}Cd_3N_8O_8$	$C_5H_6CdN_2O_2$	$C_{14}H_{22}CdN_4O_4$	$C_{15}H_{18}Hg_3N_6O_6$	$C_7H_{10}HgN_2O_2$
fw	366.66	366.66	843.67	238.52	422.74	980.09	354.74
T (K)	293(2)	293(2)	293(2)	293(2)	293(2)	293(2)	293(2)
λ (Å)	0.710 73	1.5418	1.5418	1.5418	1.5418	1.5418	1.5418
cryst syst	triclinic	monoclinic	triclinic	orthorhombic	triclinic	trigonal	monoclinic
space group	$P\bar{1}$	$P2_1/n$	$P\bar{1}$	Cmca	$P\bar{1}$	$R\bar{3}$	$P2_1/c$
a (Å)	5.025(3)	13.7766(3)	9.1060(3)	10.6603(4)	9.0097(7)	28.917(2)	10.829(1)
b (Å)	7.867(5)	5.1088(1)	9.4571(3)	17.7560(6)	10.2404(8)	28.917(2)	12.283(1)
c (Å)	8.898(8)	9.2913(2)	9.8865(3)	7.3566(3)	10.6576(8)	16.699(2)	7.2545(8)
α (deg)	103.38(6)	90	97.848(2)	90	71.096(5)	90	90
β (deg)	89.94(6)	89.885(2)	105.805(2)	90	101.242(5)	90	91.61(1)
γ (deg)	103.22(5)	90	118.620(2)	90	85.901(7)	120	90
V (Å^3)	332.6(4)	653.94(3)	682.23(4)	1392.48(9)	902.8(1)	12093(2)	964.6(2)
Z	1	2	1	8	2	18	4
ρ(calcd) (Mg m^{-3})	1.831	1.861	2.053	2.275	1.550	2.422	2.442
μ (mm^{-1})	1.66	13.3	19.1	24.7	9.9	32.1	29.9
F(000)	182	364	410	912	428	7884	648
sample size (mm^3)	0.05 × 0.10 × 0.10	20 × 8 × 0.3 (powders)	20 × 8 × 0.3 (powders)	20 × 8 × 0.3 (powders)	20 × 8 × 0.3 (powders)	20 × 8 × 0.3 (powders)	20 × 8 × 0.3 (powders)
θ range (deg)	3.00−25.30	4.50−52.50	5.00−52.50	4.50−52.50	4.00−52.50	4.00−52.50	3.00−52.50
hkl collcd	$-6 \le h \le 6$ $-9 \le k \le 9$ $0 \le l \le 10$	na	na	na	na	na	na
reflcns collcd/indep	1199/1199 [R(int) = 0.000]						
abs corr	Difabs	infinite thickness layer	infinite thickness layer	infinite thickness layer	infinite thickness layer	infinite thickness layer	infinite thickness layer
refinement method	full-matrix least-squares on F^2	full-matrix least-squares on y_i	full-matrix least-squares on y_i	full-matrix least-squares on y_i	full-matrix least-squares on y_i	full-matrix least-squares on y_i	full-matrix least-squares on y_i
data/restr/params	1199/0/88	4801/rb/35	4801/rb/42	4801/rb/22	4851/rb/71	5001/rb/46	4951/rb/32
$S(F^2)$	1.068	na	na	na	na	na	na
R1, wR2[b]	0.061, 0.152	na	na	na	na	na	na
R_{wp}, R_p, R_{Bragg}[c]	na	0.128, 0.098, 0.042	0.117, 0.088, 0.035	0.167, 0.130, 0.056	0.121, 0.090, 0.032	0.120, 0.094, 0.060	0.116, 0.087, 0.039
max/min $\Delta\rho$ (e Å^{-3})	1.5, −1.4	na	na	na	na	na	na

[a] Crystallographic data (excluding structure factors) for the seven crystal phases reported in this paper have been deposited with the Cambridge Crystallographic Data Centre supplementary publication CCDC Nos. 615255−615261. Copies of the data can be obtained free of charge on application to CCDC, 12 Union Road, Cambridge CB21EZ, U.K. Fax: (+44)1223-336-033. E-mail: deposit@ccdc.cam.ac.uk. [b] R1 = $\sum||F_o| - |F_c||/\sum|F_o|$ for reflections with $I > 2\sigma(I)$; wR2 = $[\sum[w(F_o^2 - F_c^2)]^2/\sum[w(F_o^2)^2]]^{1/2}$ for all reflections; $w^{-1} = \sigma^2(F^2) + (aP)^2 + bP$, where $P = (2F_c^2 + F_o^2)/3$ and a and b are constants set by the program. [c] $R_p = \sum_i|y_{i,o} - y_{i,c}|/\sum_i|y_{i,o}|$; $R_{wp} = [\sum_i w_i(y_{i,o} - y_{i,c})^2/\sum_i w_i(y_{i,o})^2]^{1/2}$; $R_{Bragg} = \sum_n||I_{n,o}| - |I_{n,c}||/\sum_i|I_{n,o}|$, where $y_{i,o}$ and $y_{i,c}$ are the observed and calculated profile intensities, respectively, while $|F_{n,o}|$ and $|F_{n,c}|$ are the observed and calculated structure factors. The summations run over i data points or n independent reflections. Statistical weights w_i are normally taken as $1/y_{i,o}$.

tings: 40 kV, 40 mA. Slits: DS 1.0 mm; AS 1.0 mm; RS = 0.2 mm. Indexing was by TOPAS.[17] **2**: triclinic; $a = 15.15$, $b = 9.09$, $c = 9.47$ Å; $\alpha = 118.8$, $\beta = 130.9$, $\gamma = 43.6°$ (later reduced); GOF = 43.2; space group $P\bar{1}$. **3**: orthorhombic; $a = 10.67$, $b = 17.76$, $c = 7.36$ Å; GOF = 23.5; space group (from systematic absences) *Cmca*. **4**: triclinic; $a = 10.71$, $b = 9.05$, $c = 12.24$ Å; $\alpha = 103.3$, $\beta = 127.3$, $\gamma = 78.9°$; GOF = 27.7; space group $P\bar{1}$. **5**: trigonal; $a = 28.88$, $c = 16.68$ Å; GOF = 19.9; space group (from systematic absences and successful refinement) $R\bar{3}$. **6**: monoclinic; $a = 10.90$, $b = 12.25$, $c = 7.29$ Å; $\beta = 92.1°$; GOF = 42.7; space group (from systematic absences) $P2_1/c$. The unit cell determination of **1b** from a polyphasic XRPD trace proved to be more difficult: After elimination of the peaks belonging to the contaminant minority phase **1a**, TOPAS found a primitive orthorhombic cell with $a = 13.78$, $b = 9.30$, and $c = 5.11$ Å, GOF = 85.2, and space group (from systematic absences) *Pnnm* or *Pnn*2. Only a careful examination of the peak-profile matching by the Le Bail method allowed one to detect a subtle lattice distortion, not visible as peak splitting but rather as peak shifting. Therefore, the final monoclinic cell and the $P2_1/n$ space groups reported in Table 1 were chosen, with the β angle close, but not statistically equal, to 90°. The contribution to the observed *polyphasic* XRPD trace of **1b** by the contaminant phase **1a** was refined using the structural mode derived by single-crystal methods and accounted for a mere 8% of the total.

Structure solutions were achieved by simulated annealing, using independent metal ions and acetate/pyrazole rigid fragments; once the approximate structural models were devised, the final refinements were performed by the Rietveld method (as implemented in the TOPAS suite of programs), keeping idealized rigid body moieties, helping convergence and stability. Given the complexity of the structures, rigid bodies (i.e. *constrained* fragments) for the acetate/pyrazole ligands were kept throughout the whole refinement procedure, and a few *restraints* (mostly of the antibumping type, *never released*) were added to drive the final models to covergence with chemically significant geometrical values. For the most complex structure presented here, **6**, a *rigid* trinuclear $[Hg(pz)]_3$ fragment was introduced and kept *fixed* with idealized geometry during the whole structure solution and refinement processes. The background contribution was modeled by a polynomial function; preferred orientation correction (where necessary) was applied by following the March−Dollase formulation;[18] a single isotropic B_M value was refined for Cd/Hg (lighter atoms being assigned a $B = B_M + 2.0$ Å^2 value). Further details of the crystal structure analysis can be found in Table 1. The final Rietveld refinement plots for species **1b**, **2**−**4**, **6**, and **8** are shown in Figure 8.

Solid-State ^{13}C CPMAS NMR Experiments. Solid-state NMR spectra were recorded using a Bruker AVANCE 400 spectrometer equipped with a 4 mm double bearing MAS probe. ^{13}C cross-polarization magic-angle spinning (CPMAS) spectra were recorded using recycle time of 10 s (40 s for $Zn(ac)_2 \cdot 2H_2O$), contact times of 1 ms, and spinning rate of 7 kHz (5 kHz for $Zn(ac)_2 \cdot 2H_2O$). The spectra were recorded at room temperature and were transformed using a line broadening of 20 Hz.

Results and Discussion

Synthesis and Characterization. The reaction between $[Cd(ac)_2] \cdot 2H_2O$ and pyrazole (Hpz) in hydroalcoholic solvents, in diethyl ether, or in acetonitrile, with ratios ranging from 1:2 to 1:4, yields an analytically pure compound of $[Cd(ac)_2(Hpz)_2]$ formula, **1**. Two polymorphs, **1a** or **1b**, were isolated, depending on the solvent employed during crystallization (Scheme 1). Both species are unstable in chlorinate and D_2O solutions, where ^{1}H NMR signals due to the free, neutral pyrazole ligand were observed. By heating of compound **1b** at 110 °C for 2 h, evolution of acetic acid is observed, together with the quantitative formation of a compound with $[Cd_3(ac)_4(pz)_2(Hpz)_2]$ formula, **2**. If the heating of **1b** is carried out at 180 °C and for 24 h, a species of [Cd(ac)(pz)] formula, **3**, insoluble in all organic solvents and stable to air and moisture, is at variance obtained.

Similarly, when Cd(II) acetate is treated with 3,5-dimethylpyrazole (Hdmpz) in alcoholic solvents, $[Cd(ac)_2(Hdmpz)_2]$, **4**, is quantitatively formed. By heating **4** at 110 °C, we were unable to isolate an analogous species to **2**; however, prolonged heating of **4** at 170 °C gave compound [Cd(ac)(dmpz)], **5**, the analogue of **3**. When the reaction between an excess of Hdmpz and $[Cd(ac)_2] \cdot 2H_2O$ is carried out in diethyl ether or in diethyl ether/alcohol mixtures, species containing in the crystal lattice clathrated molecules of Hdmpz, of generic $[Cd(ac)_2(Hdmpz)_2] \cdot x$Hdmpz formula (**4a,b**; **a**, $x = 2$; **b**, $x = 1$), always form. These species, present in solid polyphasic mixtures, could not be separated, and only occasionally small quantities of nearly monophasic samples could be produced. A comment on their formulation, stability, and basic structural features is reported in the Experimental Section.

Even the reaction between $[Hg(ac)_2]$ and Hpz gives different products depending on the solvents employed. If the reaction is carried out in diethyl ether/methanol mixtures, a complex species, **6**, containing the $[Hg_3(ac)_3(pz)_3]$ trimer, forms, whereas if the same reaction is performed in hydroalcoholic solvents, the polymeric derivative [Hg(ac)(pz)], **7**, is isolated. An analogous species, [Hg(ac)(dmpz)], **8**, is produced when Hdmpz is employed as an N-donor ligand.

The IR spectra of compounds **1**−**6** display the characteristic carboxylate stretching bands in the 1600−1500 cm^{-1} range. The frequency differences (Δ) between $\nu_{as}(CO_2)$ and $\nu_s(CO_2)$, in the 40−70 cm^{-1} range, suggest bridging bidentate coordination modes for the carboxylate ligands.[19] The coordination of the heterocyclic donor in an exo-bidentate fashion and the absence of coordinated neutral Hpz and Hdmpz ligands in **3**, **5**, and **6** can be deduced from the lack of the characteristic N−H stretching bands in the 3300−3000 cm^{-1} region and of heretocyclic rocking motions in the 500−450 cm^{-1} one.[20] The unidentate coordination of the carboxylate ligands in **7** and **8** can be deduced by the closer proximity of the $\nu_{as}(CO_2)$ and $\nu_s(CO_2)$ bands that in **8** are practically overlapped. All the above features (apart from the carboxylate coordination in the amorphous samples of **7**) have been later confirmed by the structure solutions and refinements (see below).

(17) *TOPAS-R*, V.3.1; Bruker AXS: Karlsruhe, Germany, 2003.
(18) Dollase, W. A. *J. Appl. Crystallogr.* **1986**, *19*, 267.

(19) Deacon, G. B.; Phillips, R. J. *Coord. Chem. Rev.* **1980**, *33*, 227. Uhlenbrock, S.; Krebs, B. *Angew. Chem., Int. Ed. Engl.* **1992**, *31*, 1647. Reim, J. J.; Krebs, B. *J. Chem. Soc., Dalton Trans.* **1997**, 3793. Ishioka, T.; Murata, A.; Kitagawa, Y.; Nakamura, K. T. *Acta Crystallogr.* **1997**, *C53*, 1029.
(20) Elguero, J. Pyrazole and their benzo derivatives. In *Comprehensive Heterocyclic Chemistry*; Katritzky A. R., Ed.; Pergamon Press: London, 1984; Vol. 5, Chapter 4.04, p 199 and references therein.

Scheme 1

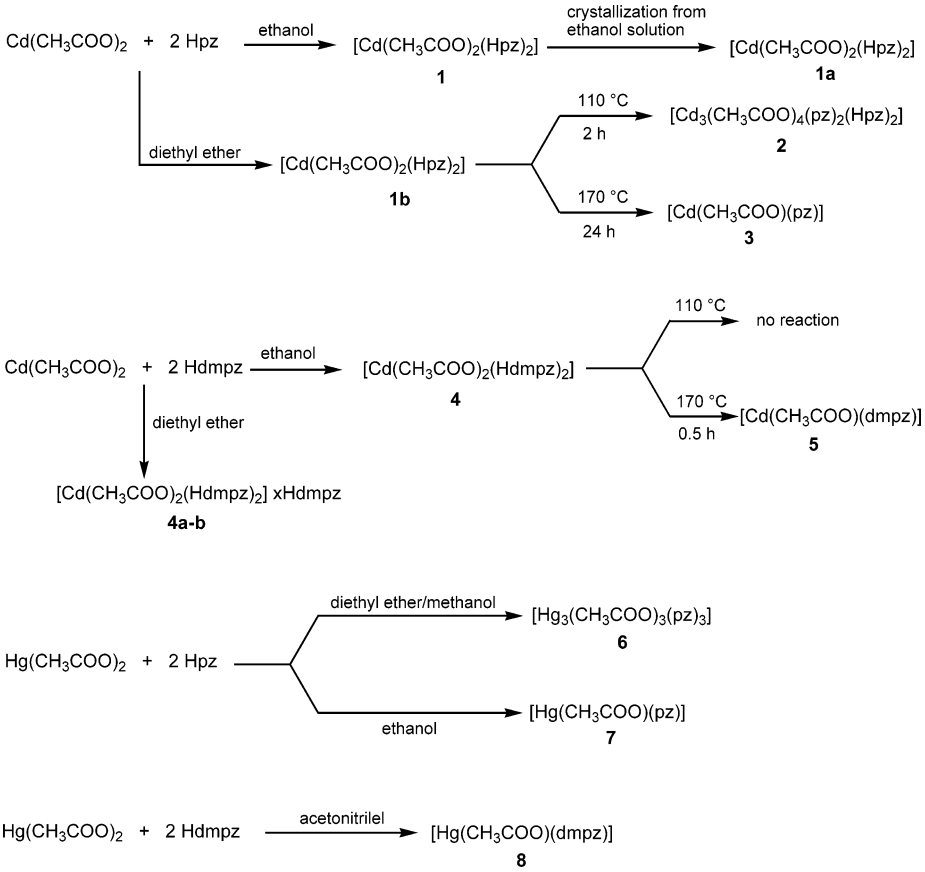

It is worth to note that IR spectra can be used to monitor the transformation of the polymeric adducts **1** and **4**, containing neutral monodentate heterocyclic ligands, further hydrogen-bonded to symmetric exo-bidentate carboxylate ligands, into the species **2**, **3**, and **5**, respectively, containing exo-bidentate azoles. Actually, in all cases a significant displacement of the carboxylate bands is observed, together with the disappearance of the N−H stretching absorption.

Aqueous solutions of compounds **1**, **4**, and **4a** and an acetonitrile solution of **6** have been also investigated by ESI MS. Likely, their polymeric nature is disrupted in solution and the formed species only vaguely resemble the parent polymers. The *m*/*z* values of prominent peaks corresponding to cadmium and mercury cations are given together with formula assignments (see Experimental Section). It is to be pointed out that, in the case of derivative **1**, four relatively abundant signals, due to the mononuclear species $[Cd(ac)(Hpz)(H_2O)_3]^+$ (*m*/*z* 295), $[Cd(ac)(Hpz)_2]^+$ (*m*/*z* 309), $[Cd(ac)(Hpz)_2(H_2O)_3]^+$ (*m*/*z* 363), and $[Cd(ac)(Hpz)_3]^+$ (*m*/*z* 377) are clearly evident, accompanied by some poorly defined signals at ca. *m*/*z* 600, whose isotopic pattern is, on the other hand, indicative of dinuclear species. In the ESI mass spectrum of compound **4a**, if one excludes the signal at *m*/*z* 97 ($[Hdmpz + H]^+$), the most evident isotopic clusters are again due to mononuclear species, $[Cd(ac)_2(Hdmpz)_2 + Na]^+$ (*m*/*z* 447) and $[Cd(ac)(Hdmpz)_3]^+$ (*m*/*z* 461), but also dinuclear ions are clearly detected $[Cd_2(ac)_3(Hdmpz)(H_2O)_3]^+$ (*m*/*z* 744) or $[Cd_2(ac)_2(dmpz)(H_2O)(Hdmpz)]^+$ (*m*/*z* 553) and $[Cd_2(ac)_4(Hdmpz)(H_2O)_2 + Na]^+$ (*m*/*z* 617). On the contrary, likely due to the low solubility of compound **4**, its ESI mass spectrum shows only the most intense signal at *m*/*z* 97, due to protonated Hdmpz, and a very weak isotopic cluster (8%) centered at *m*/*z* 447, corresponding to $[Cd(ac)_2(Hdmpz)_2 + Na]^+$.

At variance with the behavior above-reported, in the ESI mass spectrum of **6**, the major peak is that ascribed to the mononuclear species $[Hg(pz)]^+$ (*m*/*z* 269), generated by extended disruption of the trinuclear system, while isotopic clusters corresponding to di- and trinuclear ions present a low intensity and are partially superimposed one to the other, thus making their correct attribution questionable.

Crystal Structure of Triclinic [{Cd(μ-ac)$_2$(Hpz)$_2$}$_n$] (1a). This species contains hexacoordinated cadmium ions with local CdN_2O_4 geometry; each metal center bears two monodentate pyrazole ligands in trans position and is connected, by bridging acetate groups, to two other metal centers, thus generating a monodimensional chain. The asymmetric unit is composed by half a metal ion, on a crystallographic inversion center, one crystallographically independent pyrazole moiety, and an acetate group. A portion of the crystal structure is shown in Figure 1, highlighting the monodimensional nature of the polynuclear complex topology. Significant bond distances and angles are collected in the caption to the figure. The geometry about each Cd(II) ion is nearly octahedral, with the maximum deviation from the ideal angles observed for N1−Cd−O2 [95.0(2)°], the Cd−N and Cd−O bond distances lying in the narrow 2.277(7)−2.369(6) Å range. Within each chain (of $p\bar{1}$ rod

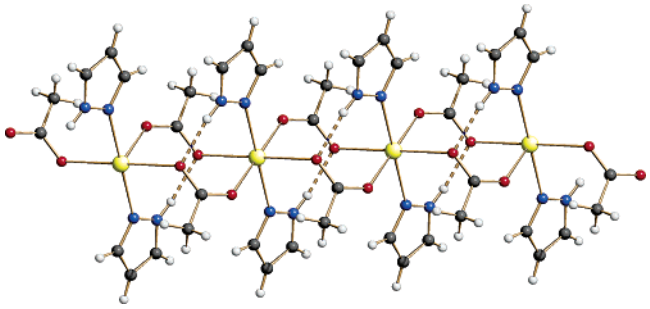

Figure 1. Schematic drawing of the mono-dimensional [{Cd(μ-ac)$_2$-(Hpz)$_2$}$_n$] polymer present in the triclinic species **1a**, running parallel to the **a** axis. Intrachain hydrogen bonds are drawn as fragmented lines. At the drawing resolution, the polymeric [{Cd(μ-ac)$_2$(Hpz)$_2$}$_n$] chains present in the monoclinic polymorph **1b** are identical. Relevant bond distances for **1a**: Cd−N 2.277(7), Cd−O 2.293(6)−2.369(6), Cd···Cd 5.025(3), N−H···O 2.76 Å.

symmetry), Cd···Cd distances of ca. 5.02 Å (the **a** vector) are present, as imposed by bridging exo-bidentate acetate groups in the *syn-anti* mode. The swinging end of the pyrazole ligands, bearing the "acidic" H(N) atom, is hydrogen-bonded in an *intra*chain manner to a neighboring acetate [(N)H···O 2.76 Å], thus forcing the polymeric chains to pack through weak(er) van der Waals interactions only.

Crystal Structure of Monoclinic [{Cd(μ-ac)$_2$(Hpz)$_2$}$_n$] (1b). Also this species contains monodimensional chains built by hexacoordinated (CdN_2O_4) cadmium ions and bridging acetate groups, each metal being further bound to two monodentate pyrazole ligands, trans to each other. As in **1a**, the asymmetric unit is composed by half a metal ion, on a crystallographic inversion center, one crystallographically independent pyrazole moiety, and an acetate group. The chains of **1b** (of $p\bar{1}$ rod symmetry as well), are essentially identical with those in **1a**, the most significant difference being their slight stretching, which raises the intermetallic contacts from ca. 5.02 Å (**1a**) to 5.11 Å (the **b** axis in **1b**). The other intrachain structural features of **1a**,**b** are comparable**,** also as a result of soft restraints introduced to stabilize the XRPD refinements. More relevant is the difference in the chains' crystal packing. In **1b**, the parallel chains run along **b** and pack in a nearly pseudohexagonal fashion. A more distorted packing is present in the triclinic polymorph: if one views down **a**, an *oblique* packing of parallel chains can be envisaged, which are slightly shifted (by *a*/4) along **a** (Figure 2). Thus, in **1b**, the *depleted* [010] preferred orientation pole, determined experimentally (see Experimental Section), can be nicely interpreted by the presence of parallel polymeric chains, likely affording a microacicular morphology of the crystallites, which would preferentially lie in the plane normal to the scattering vector. The structure of the chains present in **1b** shares some similarities with that of the polymorph **1a** (see previous paragraph) and also with that of the [{Cd(μ-ac)$_2$(Hdmpz)$_2$}$_n$] species, **4**, discussed below, with the notable exception of the location of the Cd-bound nitrogen atoms (trans *vs* cis in **4**).

Crystal Structure of [{Cd$_3$(μ_3-ac)$_4$(μ-pz)$_2$(Hpz)$_2$}$_n$] (2). This species presents two crystallographically independent cadmium ions, one (Cd1) lying on an inversion center and the other (Cd2) in general position. Both show trans-

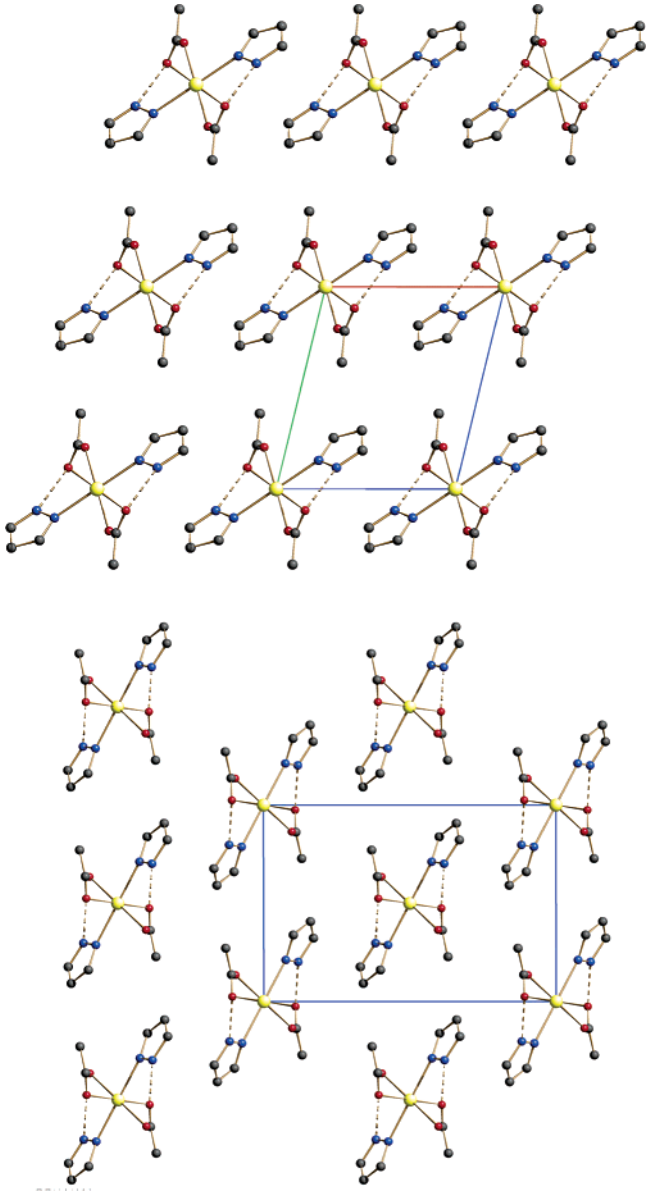

Figure 2. Schematic drawing of the crystal packing of the one-dimensional chains in the **1a,b** polymorphs. The traces of the pertinent unit cells are also drawn. Top: species **1a**, down **a** with horizontal axis **b**. Bottom: species **1b**, down **b** with horizontal axis **a**. In **1a**, the chains (running normal to the drawing) describe an oblique, two-dimensional lattice, while in **1b** a (pseudohexagonal) centered rectangular one can be envisaged.

pseudooctahedral CdN_2O_4 local geometry but are differently connected to the organic ligands: Cd1 is bound to two nitrogen atoms of two N,N′-exo-bidentate pyrazolate anions and to four distinct acetate groups, while Cd2 (also bearing four acetate moieties) binds to two neutral pyrazole ligands. A portion of the crystal structure of **2** is shown in Figure 3, where the N,N′-exo-bidentate coordination mode of the pyrazolate anion and the less common μ_3-κ_O:$\kappa_{O'}$:$\kappa_{O'}$ one of the acetate moieties can be appreciated. Relevant bond distances and angles are briefly reported in the caption to Figure 3. Different intermetallic contacts are present: Cd1···Cd2 = 3.60 Å, for a triply bridged (pz,O,O) system; Cd2···Cd2′ = 4.31 Å and Cd2···Cd2″ = 5.40 Å, for a doubly acetate-bridged system (with a *syn-anti* conformation of the O−Cd bonds), the latter being further assisted by N−H···O

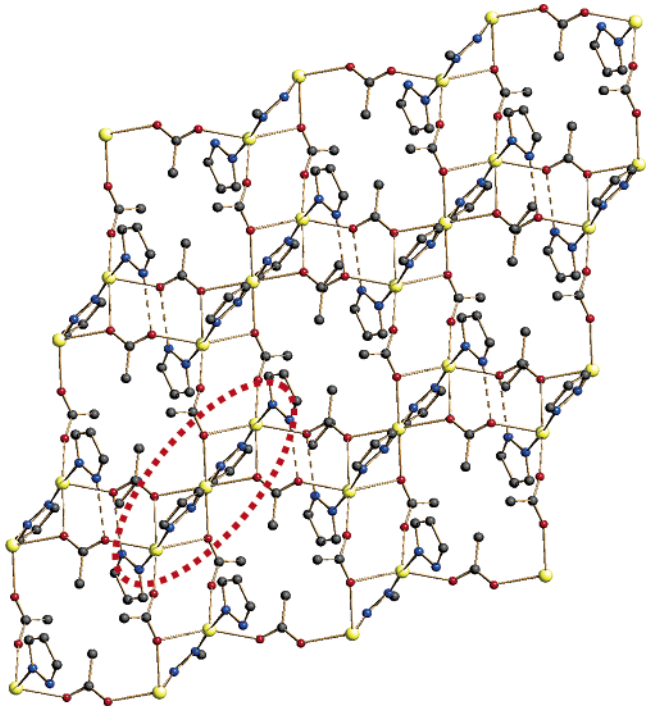

Figure 3. Schematic drawing of the two-dimensional layer present in the species **2**, the $[\{Cd_3(\mu_3\text{-ac})_4(\mu\text{-pz})_2(Hpz)_2\}_n]$ polymer, extending in the **ab** plane. Hydrogen atoms have been omitted for clarity. Hydrogen bonds drawn as fragmented lines. The linear trinuclear Cd_3 core discussed in the text is highlighted within the dashed ellipse. Relevant bond distances: Cd−N 2.284(6)−2.305(8), Cd−O 2.37(2)−2.62(2), Cd1···Cd2 3.60, Cd2···Cd2′ 4.31, Cd2···Cd2″ 5.41, N−H···O 2.88 Å.

= 2.88 Å contacts with the neighboring pyrazole ligands. The overall system, therefore, consists of two-dimensional layers (of $p\bar{1}$ symmetry) extending in the **ab** plane, while only short H···H contacts are responsible for the crystal growth in the **c** direction. Apparently, this layered structure does not morphologically induce macroscopically evident texture nor cleavage, since no preferred orientation correction was found to be necessary during our data analysis. In an alternative description, trinuclear entities of $Cd_3(pz)_2(Hpz)_2$ formulation (highlighted in Figure 3) are extensively interconnected, in the crystal, by the bridging acetate groups. Such a trinuclear core is not new, being a portion of already known azolate-bridged systems, where intermetallic interactions range from 3.71[21] to 4.28 Å.[22]

Crystal Structure of $[\{Cd(\mu\text{-ac})(\mu\text{-pz})\}_n]$ (3). This species contains tetracoordinated (CdN_2O_4) cadmium ions bridged by acetates and pyrazolates, both in their exo-bidentate mode. A portion of its crystal structure is shown in Figure 4. Two stereochemically different Cd···Cd interactions are present: those bridged by two exo-bidentate acetate groups in the *syn-syn* mode (ca. 3.73 Å) and those bridged uniquely by pyrazolate anions (ca. 4.01 Å, i.e. slightly larger than those observed in the long known homoleptic $[\{Cd(\mu\text{-pz})_2\}_n]$ 1D polymer,[23] 3.96 Å). The geometry about each Cd(II) ion is heavily distorted from the ideal tetrahedral

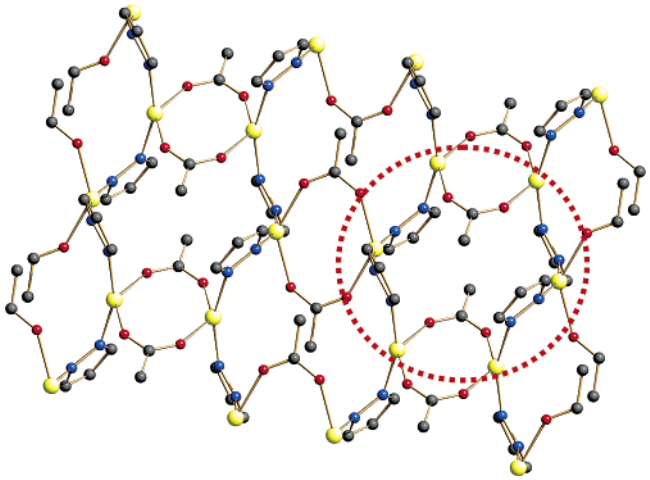

Figure 4. Schematic drawing of the two-dimensional layer present in the species **3**, the $[\{Cd(\mu\text{-ac})(\mu\text{-pz})\}_n]$ polymer, extending in the **ab** plane. Hydrogen atoms have been omitted for clarity. The $Cd_6(ac)_2(pz)_4$ ring discussed in the text is highlighted within the dashed circle. Relevant bond distances and angles: Cd−N 2.235(9), Cd−O 2.268(13), Cd···Cd 3.73−4.01 Å; N−Cd−N 161.3(5), N−Cd−O 88.6(5)-98.0(4), O−Cd−O 138.3(3)°.

values, with a rather large N−Cd−N angle of 161°, probably because of the geometrical constraints imposed by the polymeric nature and periodicity restraints. Similar anomalous Cd(II) geometries, although rare, are not new: see for example the crystal structures of the mononuclear $Cd(Pcy_3)_2$-(2,6-F-phenolate)$_2$ and of the $Cd(CH_3)_2$(dioxane) polymer, where angles up to 173.0° are found.[24] The overall structure is polymeric and contains two-dimensional layers, stacked along **b**, of idealized *p*2/*m*2/*c*2/*a* symmetry, interacting only through weak H···H van der Waals contacts. The experimental observation of a preferred orientation [*0k*0] pole thus finds a clear structural explanation. Within each layer, $[Cd_2(ac)_2]^{2+}$ fragments can be envisaged, which are interconnected by four pyrazolates to other (symmetry-related) dimers, thus forming Cd_6 *fused* centrosymmetric cycles (see Figure 4), where the cadmium ions (located at the nodes of a honeycomb framework) are bridged by four pyrazolates and two pairs of acetate ligands. Interestingly, the recently reported $[\{Zn(\mu\text{-ac})(\mu\text{-pz})\}_n]$ polymer,[8] which also displays two-dimensional layers built on bridging acetates and pyrazolates, is not isomorphous with **3**; indeed these two species, while sharing an approximate distribution of the metal atoms within the layers, show a different decoration of the M···M contacts, with mutual reversal of the acetate/pyrazolates positions, the zinc species containing *acetate*-bridged $[Zn_2(pz)_2]^{2+}$ fragments and *not pyrazolate*-bridged $[Zn_2(ac)_2]^{2+}$ ones.

Crystal Structure of $[\{Cd(\mu\text{-ac})_2(Hdmpz)_2\}_n]$ (4). This species contains hexacoordinated cadmium ions, bridged by exo-bidentate acetate groups, in the less common *syn-anti* coordination mode, the intermetallic distance approaching 4.98 Å (to be compared with 5.02 and 5.11 Å in **1a**,**b**, respectively). The coordination sphere of each Cd ion is completed by two nitrogen atoms of two different *neutral*

(21) Yi, L.; Ding, B.; Zhao, B.; Cheng, P.; Liao, D.-Z.; Yan, S.-P.; Jiang, Z.-H. *Inorg. Chem.* **2004**, *43*, 33.
(22) Xuan-Wen, L. *Acta Crystallogr.* **2005**, *E61*, m1777.
(23) Masciocchi, N.; Ardizzoia, G. A.; Maspero, A.; LaMonica, G.; Sironi A. *Inorg. Chem.* **1999**, *38*, 3657.
(24) Darensbourg, D. J.; Wildeson, J. R.; Yarbrough, J. C.; Taylor, R. E. *Inorg. Chem.* **2001**, *40*, 3639. Almond, M. J.; Beer, M. P.; Drew, M. G. B.; Rice, D. A. *J. Organomet. Chem.* **1991**, *421*, 129.

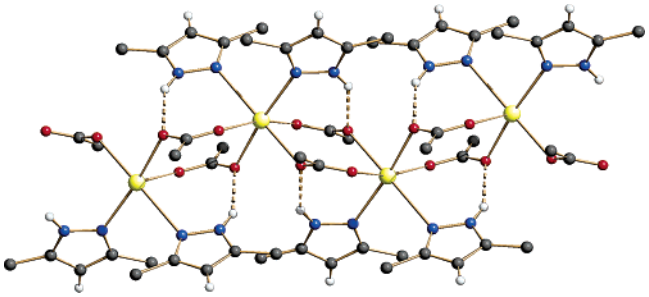

Figure 5. Schematic drawing of the one-dimensional [{Cd(μ-ac)$_2$-(Hdmpz)$_2$}$_n$] chain of **4**, with intramolecular hydrogen bonds represented with dashed lines. Relevant bond distances and angles: Cd−N 2.30(2)−2.58(2), Cd−O 2.19(4)−2.46(2), Cd···Cd 4.97−4.99 Å; N−Cd−N 83.1(9)°; trans angles at Cd N−Cd−O 172(1)−174(1), O−Cd−O 163(1)°.

dimethylpyrazole ligands, cis to each other (Figure 5). At variance, the unsubstituted pyrazole analogues (**1a**,**b**), although bearing some resemblance to species **4**, show a very distinct local geometry, with trans CdN_2O_4 coordination. The swinging end of the each Hdmpz ligand bears "acidic" hydrogen atoms, involved in *intra*molecular hydrogen bond interactions with the anti oxygen atoms of the bridging acetates (N−H···O ca. 2.81−2.85 Å). All together, one-dimensional chains, running along **a**, are formed, which do not show any specific short interaction with the neighboring ones, the crystal packing of parallel bundles being stabilized (mostly) by H···H van der Waals contacts; accordingly, the refined texture parameter indicates a significantly *depleted* [100] pole.

Crystal Structure of [{Hg$_3$(μ-ac)$_3$(μ-pz)$_3$}$_n$] (6). The rhombohedral structure of **6** is rather complex. Each unit cell (see Figure 6) contains 18 "isolated" trinuclear [Hg$_3$-(pz)$_3$]$^{3+}$ fragments, in which the Hg(II) ions are essentially linearly coordinated; these trimers are interconnected by bridging acetate groups which, interacting with the metal centers in the plane normal to the N−Hg−N vectors, with Hg−O distances in the 2.29−2.47 Å range (see insert at the bottom of Figure 6), complete the metal coordination to an idealized SF_4 stereochemistry and raise the overall network dimensionality to 3D. Possibly, a number of longer Hg···O contacts, up to ca. 3.00 Å, are further stabilizing this complex crystal structure (leading to some trigonal bipyramidal Hg atom coordination).

Crystal Structure of [{Hg(ac)(μ-κ_C:κ_N-Hdmpz)}$_n$] (8). This species contains linearly coordinated mercury(II) ions, bridged by (C-deprotonated) Hdmpz ligands through their N and C4 atoms. It is worth noting that such uncommon feature is unambiguously determined by (i) the 1,3 bridging connectivity of the pyrazolate ring, (ii) the location of the branching methyl groups, and (iii) the solid-state NMR features reported below. The coordination sphere at the Hg(II) ions is further completed by a weakly bound monodentate acetate group [Hg−O 2.81(3) Å], affording a one-dimensional polymer build upon a sequence of C-mercuriated Hdmpz ligands (separating Hg ions by about 6.16 Å), and radially swinging acetate groups. A portion of the crystal structure is shown in Figure 7. A nearly linear geometry is observed for the N−Hg−C angle [172(1)°], the [{Hg(μ-Hdmpz)}$_n$] chain possessing only (crystallographically imposed) 2_1 symmetry. The refined Hg−C bond distance [2.07(2) Å] well compares with those of the few other known mercuriated heterocycles of this kind, mostly imidazoles; indeed, within this class, Hg−C values lie in the narrow 2.00−2.09 Å range.[25] A survey in the CSD database indicated that, among simple C-mercuriated pentatomic azaaromatic

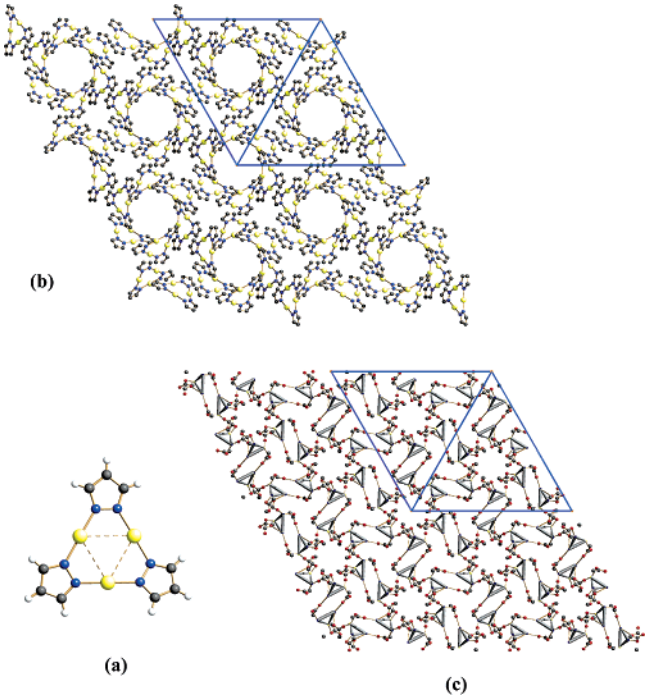

Figure 6. Schematic drawings of the complex crystal structure of **6**, the [{Hg$_3$(μ-ac)$_3$(μ-pz)$_3$}$_n$] species, crystallizing in the rhombohedral $R\bar{3}$ space group. *Isolated* [Hg$_3$(pz)$_3$]$^{3+}$ fragments (a) pack in space as shown in (b), down [001], where acetate groups are omitted. At variance, (c) shows [Hg$_3$-(pz)$_3$]$^{3+}$ triangles (black) interconnected by the bridging acetate groups. Hydrogen atoms have been omitted in (b) and (c) for clarity.

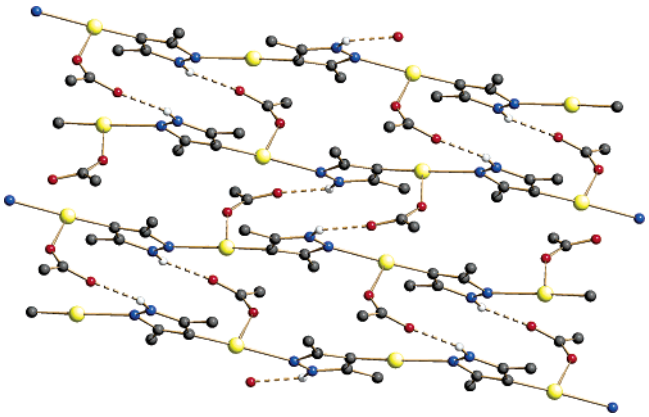

Figure 7. Schematic drawing of the one-dimensional chains present in the species **8**, the C-metalated [{Hg(ac)(μ-κ_C:κ_N-Hdmpz)}$_n$] polymer, winding up the **b** axis. Parallel chains interact through hydrogen bonds (drawn as fragmented lines) leading to two-dimensional sheets extending in the **bc** plane. Relevant bond distances and angles: Hg−C 2.07(2), Hg−N 2.30(2), Hg−O 2.81(3), N−H···O 2.83(3) Å; C−Hg−N 172(1)°.

(25) With the notable exception of [$C_{16}H_{16}HgN_8$](PF_6)$_2$ (Lee, K. M.; Chen, J. C. C.; Lin, I. J. B. *J. Organomet. Chem.* **2001**, *617*, 264. Range of Hg−N distances: 1.97−2.22 Å), which was *incorrectly* refined in the acentric *Cc*, instead of the correct centrosymmetric *C*2/*c* space group, thus being somewhat distorted by heavy parameter correlations (Marsh, R. E. *Acta Crystallogr.* **2004**, *B60*, 252).

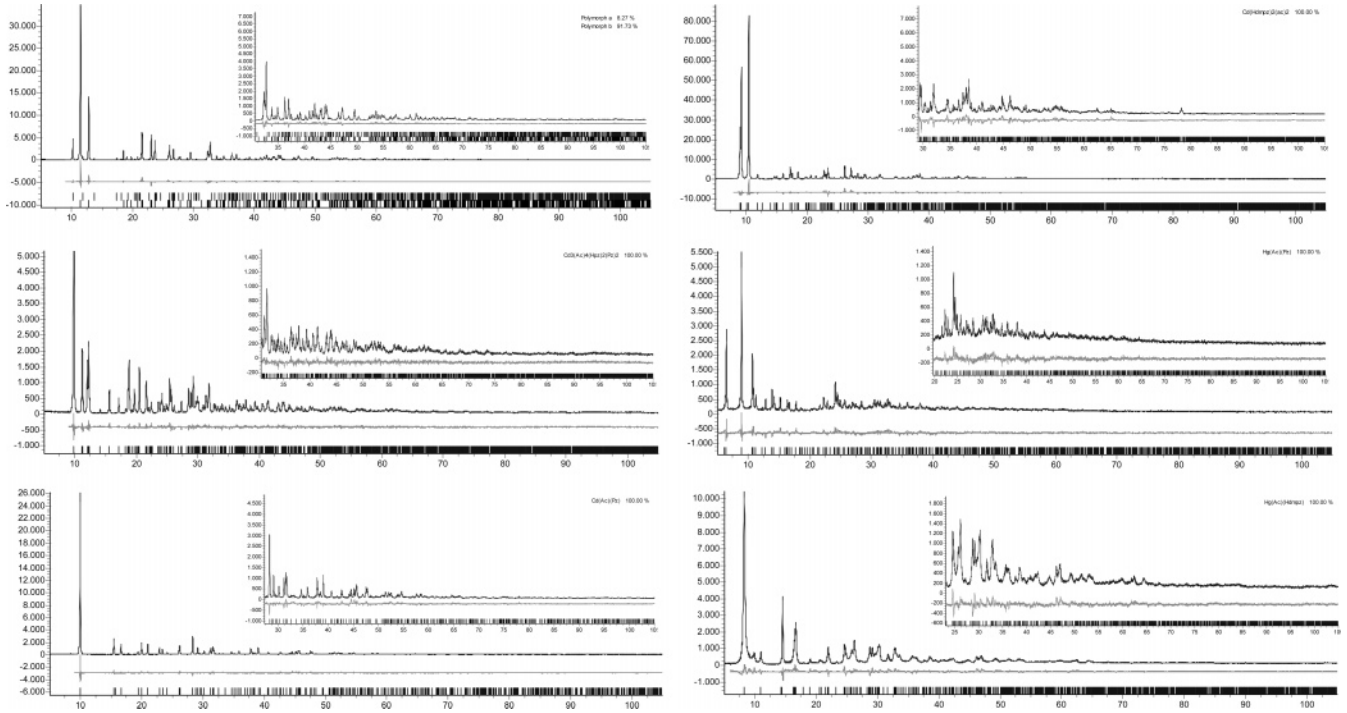

Figure 8. Final Rietveld refinement plots for species **1b**, **2**−**4**, **6**, and **8**, with peak markers and difference plot. The high angle regions have been magnified (5×, 10× for **4**) in the inserts. A few weak peaks from the aluminum sample holder at high angles can be also appreciated.

ligands, only one pyrrole[26] (Hg−C 2.01 Å) and less than 20 C-bound imidazoles have been structurally characterized; consequently, that of **8** appears to be the first mercuriated pyrazole-containing structure ever known. Interchain hydrogen bonds between the free oxygen atoms of the acetate groups and the Hdmpz nitrogen atoms not involved in metal coordination [N−H···O 2.83(3) Å] couple neighboring chains stacked in the **c** direction (Hg···Hg 3.73 Å), leading to the formation of two-dimensional layers extending in the **bc** plane. As in **2** and **4**, only H···H van der Waals contacts (mostly of the acetate groups) are present between the building units of the crystal, here the 2D layers of $p2_1/c$ symmetry.

Solid-State ^{13}C CPMAS NMR Spectroscopic Properties. To probe the magnetic properties of the ^{13}C nuclei on the above-described polymers, we measured their solid-state NMR chemical shifts on bulk solid samples. This allowed us both to confirm the crystal structure symmetry derived from complex XRPD traces and to validate a tool for assessing the nature and stereochemistry of hitherto structurally uncharacterized solid, amorphous or poorly crystalline, samples. The relevant data are collected in Table 2, in which the different resonance values of the heterocyclic carbon atoms can be properly correlated with the nature of the pyrazole ligands, either anionic, exo-bidentate, or even C-metalated, as witnessed by the 10 ppm low-field shift of the ^{13}C resonances. Of particular relevance is the deshielding of the Hg-bound carbon atom in **8** (118.8 ppm), which confirms its unique environment (similar changes of the *solution* ^{13}C NMR resonances have been observed upon mercuriation of aromatic rings by Vicente et al.[27]).

This is particularly relevant in addressing the *local* coordination properties of the Hg(II) ions in species **7**. Indeed, despite the many attempts and crystallization procedures, **7** invariably precipitated as an intractable white solid with nearly amorphous XRPD traces (a few broad peaks are however present, indicating that at least some local ordering occurs). Thus, in the absence of (poly)crystalline materials amenable to diffraction characterization, the 116.1 ppm resonance observed in the ^{13}C CP-MAS NMR spectrum for species **7** suggests, also in this case, that C-mercuriation of the pyrazole rings has occurred.

Comparative Structural Analysis. The structures reported above can be meaningfully compared with the zinc analogues, allowing the observation of a number of different trends.

(i) Zinc pyrazolates and pyrazole/acetates show invariably tetracoordinated metal ions, of the ZnN_xO_{4-x} kind. At variance, the cadmium analogues, presented above, are mostly hexacoordinated. Within this class, only $[\{Cd(\mu\text{-}pz)_2\}_n]$[23] and $[\{Cd(\mu\text{-ac})(\mu\text{-pz})\}_n]$ show (pseudo)tetrahedral geometry, with CdN_4 or CdN_2O_2 environments, respectively. Even more dramatic is the stereochemical change observed on passing to the hitherto known Hg(II) derivatives. $[\{Hg(pz)_2\}_n]$ contains linearly coordinated Hg(II) ions, with long ancillary Hg−N interactions in the plane normal to the main N−Hg−N vector.[23] The Hg(II) mixed-ligand species discussed above maintain these basic features, with looser interactions with the acetate ligands rather than with pyrazolate groups.

(26) Hubler, K.; Hubler, U.; Roper, W. E.; Wright, L. J. *J. Organomet. Chem.* **1996**, *526*, 199.

(27) Vicente, J.; Abad, J.-A.; Rink, B.; Hernández, F.-S.; Ramírez de Arellano, M. C. *Organometallics* **1997**, *16*, 5269.

Table 2. ^{13}C CPMAS NMR Chemical Shifts for the Acetate and Pyrazole Ligands in Species **1b**, **2**, and **6**−**8** and Similar Species Taken as Reference, Where Bold Values Refer to C-Metalated Pyrazoles

species	**C**H_3COO	CH_3**C**OO	C3,C5	C4	**C**H_3−C	ref
Hpz			128	107		c
			139			
Hdmpz			141.0	104.9	11.8[a]	d
			146.2			
[Zn(ac)$_2$·2H_2O]	20.0	184.0				this work
[Zn(μ-ac)(μ-pz)(Hpz)]$_2$	22.7	180.5	132.4	104.6		this work
			137.7	105.5		
			139.7			
			140.6			
[{Zn(μ-ac)(μ-pz)}$_n$]	24.2	182.2	140.1[a]	106.3		this work
[{Cd(μ_3-ac)$_2$(Hpz)$_2$}$_n$], **1b**	25.5	182.7	129.7	107.2		this work
			139.7			
[{Cd$_3$(μ-ac)$_4$(μ-pz)$_2$(Hpz)$_2$}$_n$], **2**	25.6[a]	178.2	128.9	102.7		this work
		181.6	138.5	104.0		
			140.4[a]			
[{Hg$_3$(μ-ac)$_3$(μ-pz)$_3$}$_n$], **6**	21.9	177.1	134.7	105.2		this work
	24.7	180.8 (w)	148.3			
	28.1					
[Hg(ac)(pz)], **7b**	24.6	176.4	149.2	116.1		this work
	28.2					
[{Hg(ac)(μ-κ_C:κ_N-Hdmpz)}$_n$], **8**	24.2	181.2	147.8	118.8	13.5[a]	this work
			155.7			

[a] 2×. [b] Broad. [c] Elguero, J.; Fruchier, A.; Pellegrin, V. *J. Chem Soc., Chem. Commun.* **1981**, 1207. [d] Baldy, A.; Elguero, J.; Faure, R.; Pierrot, M.; Vincent, E. J. *J. Am. Chem. Soc.* **1985**, *107*, 5290.

(ii) The isomorphic nature of the 1D [{Zn(μ-pz)$_2$}$_n$] and [{Cd(μ-pz)$_2$}$_n$] polymers is not maintained in the mixed-ligand layered systems [{M(μ-ac)(μ-pz)}$_n$] (M = Zn, Cd), where, despite of the similar disposition of the metal atoms, the decoration of the polygonal edges is totally different.

(iii) A crystalline phase, **6**, and an amorphous material, **7**, possessing the same [Hg(ac)(pz)] stoichiometry do not differ, as often found, in the supramolecular arrangement[28] or by the oligomer/polymer dichotomy;[29] rather, two differently deprotonated pyrazoles are present in these two species, one in the common N,N′-exobidentate form and the other in the C-metalated one. This latter coordination mode, evidenced by solid-state NMR spectra, is counterparted by an unequivocal structure determination of the dmpz analogue.

Conclusions

In this paper we have presented the preparation and structural analysis, mostly from powder diffraction data, of a number of pyrazole/pyrazolate derivatives of cadmium and mercury acetates. This complements our previous studies of similar zinc oligomeric and polymeric species, which showed a rich chemistry and interesting (thermally or chemically induced) interconversion processes. Differently from what originally reported by us on analogous Cu(II) systems,[6] and for the recently communicated Zn(2,2′-bipyridyl)(4-dimethylaminobenzoate)$_2$ species,[30] no evident gas/liquid sorption properties were ever noticed. However, further work on these systems can be anticipated in the direction of probing other functional properties (luminescence and catalysis), as nicely reported, for similar species, by the pioneering work of Fujita and co-workers.[31]

Our systematic study, although still lacking completeness (given the enduring absence of a structural model for the **4a**,**b** and **5** adducts), coupled with solid-state NMR measurements, allowed the determination of the C-mercuriated nature of an amorphous sample, once a full ^{13}C CP-MAS NMR spectral comparison was made.

As often reported, powder diffraction analysis can only give approximate structural models, which need the extensive use of rigid bodies and of geometrical constraints to allow convergence to a chemically reasonable model. This is particularly true when (organic or organometallic) molecular or low-dimensional polymeric compounds are studied, since the complexity of their diffraction patterns, the low scattering power of the light atoms, and the high thermal motion (compared to conventional "ionic" or inorganic samples) obscure many structural details. Accordingly, in this paper, the overall connectivity and the crystal packing are deeply discussed, and *no* effort has been put in overinterpreting intrinsically "blurred" structural features. Needless to say, a low-accuracy structure is always better than *no structure* at all.

Acknowledgment. Universities of Camerino, Insubria, and Padova, Fondazione CARIPLO, and Fondazione Provinciale Comasca are acknowledged for funding.

Supporting Information Available: Full crystallographic data in CIF format. This material is available free of charge via the Internet at http://pubs.acs.org.

IC061349B

(28) As in the **1a**,**b** couple or in the α- and β-[{Cu(μ-pz)}$_n$] phases: Masciocchi, N.; Moret, M.; Cairati, P.; Sironi, A.; Ardizzoia, G. A.; La Monica G. *J. Am. Chem. Soc.* **1994**, *116*, 7668.

(29) As in the [{Ag(μ-pz)}$_n$] and [{Ag(μ-pz)}$_3$] phases: see previous reference.

(30) Das, S.; Bharadwaj, P. K. *Inorg. Chem.* **2006**, *45*, 5257.

(31) Fujita, M.; Kwon, Y. J.; Washizu, S.; Ogura, K. *J. Am. Chem Soc.* **1994**, *116*, 1151.